

## Model Predictive Controlled Novel Supermaneuverable Tricopter Design

Afework Alemu Zeudu<sup>1</sup>, Yemane Gebremichael Gebremedhin<sup>2</sup>, Yohannes Kiros Amare<sup>1</sup>, Nebyat Gebregziabhier Weldearegay<sup>1</sup>

<sup>1</sup>Mekelle University, Mekelle, Ethiopia, [afeworkzalemu@gmail.com](mailto:afeworkzalemu@gmail.com), [yohannes.kiros@mu.edu.et](mailto:yohannes.kiros@mu.edu.et),  
[nebyat.gebregziabhier@mu.edu.et](mailto:nebyat.gebregziabhier@mu.edu.et)

<sup>2</sup>Aksum University, Aksum, Ethiopia, [yemanegm1101@gmail.com](mailto:yemanegm1101@gmail.com)

Corresponding author: [afeworkzalemu@gmail.com](mailto:afeworkzalemu@gmail.com)

Received 18 April 2025; revised 10 May 2025; accepted 20 June 2025

### Abstract

This paper presents the design, modeling, and control of a novel supermaneuverable tricopter (SMT) featuring dual-axis thrust vectoring on each of its three rotors. Unlike conventional tricopters, which face under-actuation and yaw-pitch coupling, the SMT offers over-actuation with nine independent control inputs for six degrees of freedom. This allows complete decoupling of motion and enables agile maneuvers in complex environments, which is essential for modern UAV applications. The control system is based on a Model Predictive Controller (MPC), formulated to exploit the SMT's over-actuation by optimizing control inputs over a finite prediction horizon while satisfying state and input constraints. The controller uses a linear discrete model to forecast behavior and generate real-time optimal trajectories. Simulation results demonstrate that the MPC effectively tracks complex reference trajectories with high precision, without violating actuator or dynamic constraints. The proposed implicit MPC implementation demands only modest computational resources, making it deployable on embedded systems without the need for conversion to explicit MPC. The combination of minimal processing overhead, trajectory tracking accuracy, and constraint adherence confirms the practicality of the approach.

**Keywords:** Decoupled, MPC, Novel, Over-actuation, Supermaneuverable, Tricopter.

### 1. Introduction

Unmanned Aerial Vehicles (UAVs) have become indispensable across a diverse array of domains, ranging from entertainment monitoring and photography to logistics, disaster response, and military operations (Floreato & Wood, 2015; Tahir et al., 2025). Their rapid technological maturation and operational reliability have catalyzed their integration into both civilian and defense infrastructures (Mohanty et al., 2023). Notably, the ongoing Russia-Ukrainian conflict has served as a real-world catalyst for the accelerated deployment and tactical evolution of UAVs, underscoring their strategic utility and adaptability across diverse and dynamic environments (Kunertova, 2024). Consequently, UAVs now manifest in a wide spectrum of designs and configurations, each tailored to meet specific mission

profiles and operational constraints.

Among these, tricopters have emerged as a compelling alternative to conventional quadrotors and hexarotors, offering advantages in mechanical simplicity, reduced component count, and lower power consumption(Sai, n.d.). Their inherently compact structure, coupled with enhanced agility, makes them particularly suitable for constrained or energy-sensitive missions(Mohamed & Lanzon, 2012a). However, despite these advantages, traditional tricopters face enduring limitations, most notably, an inherent asymmetry in thrust configuration leading to persistent yaw instability(Barua & Maneeshwar, n.d.). Unlike quadcopters, which utilize counter-rotating propeller pairs to cancel net torque, tricopters generate uncompensated yaw torque due to their tri-rotor arrangement(Sai, n.d.).

Beyond yaw instability, tricopters and other multirotor platforms are fundamentally constrained by under-actuation and control coupling. With only four effective control inputs (three thrust magnitudes and a single yaw mechanism) for six degrees of freedom, traditional tricopters cannot independently control translation and orientation(Sai, n.d.). This results in coupled dynamics, where generating horizontal motion necessitates body tilting(Mohamed & Lanzon, 2012a).

Early tricopter configurations, often termed pure tricopters, feature three fixed propellers arranged in a Y or T frame and can achieve vertical takeoff, landing, and hovering. However, they suffer from severe control coupling between the pitch and yaw axes due to asymmetric rotor placement, rendering them largely obsolete for practical applications(Barua & Maneeshwar, n.d.; Mohamed & Lanzon, 2012a; Sai, n.d.). To address this, various configurations have emerged. One common approach introduces a servo-actuated rear rotor capable of thrust vectoring, effectively decoupling yaw from pitch and enhancing maneuverability with minimal mechanical complexity(Abara et al., 2020; Ding & Lu, 2021; Hao et al., 2022). Another alternative employs a coaxial rear rotor system with counter-rotating propellers to neutralize yaw torque without requiring a tilting mechanism(Arroyo et al., 2021; Ding & Lu, 2021; Mohamed & Lanzon, 2012b; Peksa & Mamchur, 2024). Further advancements include fully coaxial tricopters with six propellers for improved torque balance, though these designs trade off compactness and efficiency due to increased mass and power consumption(Ding & Lu, 2021; Floreano & Wood, 2015; Mehndiratta & Kayacan, 2018; Mohanty et al., 2023).

More recent developments focus on tiltrotor and vectoring mechanisms. Tiltrotor tricopters integrate front rotor tilting to achieve forward thrust without pitching the body, often combined with a servo-actuated tail rotor to manage yaw-pitch coupling(Barua & Maneeshwar, n.d.; Ding & Lu, 2021; Mohamed & Lanzon, 2012b; Sai, n.d.). In contrast, fully tilting tricopters equip all three propellers with independent vectoring, providing greater control authority and the potential to eliminate traditional yaw control systems(Chen & Jia, 2020; Cortés & Egerstedt, 2017; Nam et al., 2020; Qin et al., 2025). Despite these innovations, existing tricopter configurations remain underactuated and directionally constrained, limiting omnidirectional movement and agility.

To overcome these structural and control limitations, this research introduces a supermaneuverable tricopter design that leverages a 2-axis thrust vectoring on each rotor via dual revolute joints. This design paradigm transitions the tricopter from an under actuated to an over actuated system, providing nine independent control inputs, three thrust magnitudes and six vectoring angles, for six degrees of freedom. This over-actuation is a foundational enabler of decoupled control, allowing the vehicle to perform agile, precise maneuvers in complex 3D environments while maintaining orientation stability and energy efficiency(Qin et al., 2025; Sheng & Sun, 2016).

The concept of supermaneuverability, originally developed in the context of high-performance fighter aircraft, denotes a platform's ability to exceed the conventional aerodynamic limits of flight, achieving rapid, precise changes in orientation and trajectory. Transposing this capability into rotorcraft, particularly UAVs, represents a transformative leap in aerial mobility(Chen & Jia, 2020). Supermaneuverability enables

navigation through narrow, cluttered, or dynamically changing spaces with a degree of freedom previously unattainable in traditional multirotor (Cortés & Egerstedt, 2017). This is critical for a growing array of UAV applications, including urban package delivery, structural inspection of confined or hazardous areas, and search-and-rescue missions in collapsed or debris-filled environments (Landry et al., 2016; Valsan et al., 2020).

Moreover, the ability to achieve arbitrary orientations confers not only enhanced agility but also superior resilience in turbulent conditions. In scenarios such as navigating partially collapsed buildings, maintaining hover in strong wind gusts, or executing precision landings in cluttered urban environments, the proposed supermaneuverable tricopter offers a significant operational advantage over existing UAV platforms (Michael et al., 2010).

## 2. Methods and Techniques

### 2.1 Methods

The research followed a model-based approach to design, model, and control a novel supermaneuverable tricopter (SMT). The work began with conceptualizing a rotorcraft configuration incorporating dual-axis thrust vectoring at each rotor to achieve over-actuation. The dynamic behavior of the tricopter was mathematically represented using Newton–Euler formulations for translational and rotational dynamics, combined with kinematic transformation matrices to relate body-frame and inertial-frame motions. The equations were expressed in state-space form to enable advanced control design.

The developed model was discretized using numerical integration (fourth-order Runge-Kutta) for simulation purposes. The control strategy was implemented using implicit Model Predictive Control (MPC), which solved a finite-horizon optimal control problem at each sampling step while enforcing actuator and state constraints.

Simulations were conducted in MATLAB/Simulink, with scenarios involving complex reference trajectories specifically a 3D helical path to validate precision tracking under realistic constraints. Performance metrics included tracking accuracy, computational efficiency, and constraint compliance.

### 2.2 Techniques

**Dual-axis thrust vectoring:** Introduced at each rotor via two revolute joints to provide nine independent control inputs for six degrees of freedom, enabling decoupled translational and rotational control.

**Newton–Euler rigid body modeling:** Applied for dynamic formulation, incorporating rotor thrust and torque as quadratic functions of rotor angular velocity.

**State-space modeling:** Facilitated the integration of the tricopter’s full dynamic behavior into the control framework.

**Model Predictive Control (MPC):** Used for predictive, constraint-aware optimization of control inputs over a defined prediction horizon.

**Simulation in MATLAB/Simulink:** Validated controller performance and system behavior under a helical trajectory tracking tasks with the following equation.

$$x = 20 * \cos(0.1 * t) \tag{1}$$

$$y = 20 * \sin(0.1 * t) \tag{2}$$

$$z = t \tag{3}$$

### 2.3 Design and Analysis

By integrating two rotational degrees of freedom at each propeller, the system achieves complete decoupling between translational and rotational motion. Specifically, thrust vectoring independently

governs pitch, roll, and yaw, eliminating the inherent coupling typical in conventional multirotor. As a result, the vehicle can achieve translational motion in any direction without requiring a change in body orientation, thereby supporting arbitrary attitude control at any position in space.

The Tricopter as shown in Figure 1 possesses nine independent control inputs, which exceeds the six degrees of freedom (DoF) required to fully define the position and orientation of a rigid body in 3D space. This over-actuation enables multiple control strategies to achieve a given motion, enabling flexibility for optimization with respect to energy efficiency, responsiveness, or disturbance rejection.

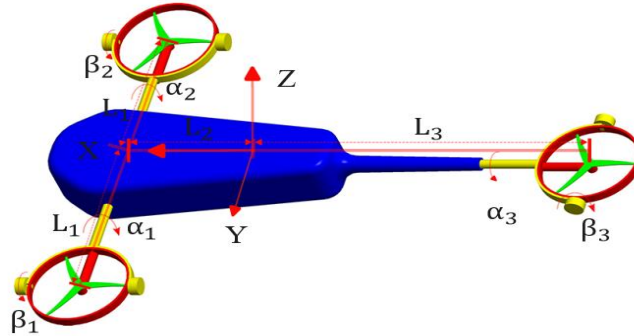


**Fig. 1.** Novel Supermaneuverable Tricopter Model

The result is a vehicle capable of achieving arbitrary orientations and movements regardless of its current attitude, significantly expanding its operational envelope. This capability enables highly agile behavior in confined environments, accurate reorientation for real-time target tracking, and collision avoidance in cluttered or dynamic settings. Furthermore, the ability to independently command both position and orientation supports advanced trajectories that involve simultaneous translation and rotation, laying the groundwork for next-generation aerial robotic systems capable of navigating unstructured, highly constrained environments with high precision.

The proposed tricopter configuration comprises two front-mounted propellers rotating in the clockwise direction and a single rear-mounted propeller rotating counterclockwise. The geometric layout is such that the distance from the center of mass (CoM) to each front propeller is denoted as  $L_2$ , while the distance to the rear propeller is  $2L_2$  (labelled as  $L_3$ ). This ratio ensures a net-zero rotational moment about the center of mass.

The Supermaneuverable Tricopter (SMT) demonstrates a significantly enhanced maneuvering capability relative to conventional platforms, those surveyed in the Literature review. It possesses the ability to execute any maneuver achievable by earlier designs, and more so, owing to its over actuated design. Notably, for a given motion such as yaw, the SMT can achieve the desired response through multiple independent control strategies, like:

- By generating differential thrust in the X-axis or Y-axis using the front propellers with different or opposing twist angles,
- By changing the twist angle of the rear propeller,
- Through coordinated actuation of all propeller twist angles, or
- By varying the propeller speeds of the front propellers and the rear propeller.

This multiplicity of actuation pathways introduces functional redundancy, enabling the selection of an optimal control strategy based on various performance criteria such as energy efficiency, response time,

control simplicity, trajectory optimality, or power consumption. As a result, the system can dynamically adapt to mission requirements or environmental constraints in real-time.

Furthermore, the inherent redundancy renders the platform fault-tolerant in the event of actuator failure or degraded performance, alternative control modes remain available to accomplish the intended maneuver. This contributes to the system's robustness and enhances its operational reliability.

## 2.4 Supermaneuverable Tricopter Modeling

The Supermaneuverable Tricopter is mathematically modeled using the Newton-Euler formulation, which provides a comprehensive framework for describing the translational and rotational dynamics of rigid bodies (Murray et al., 1994; Siciliano et al., 2009a). Under the standard rigid body assumptions, the tricopter's structure is non-deformable, its mass distribution remains constant, and it experiences no internal vibrations or elastic deformations (Bouabdallah & Siegwart, 2007). The equations of motion are derived by applying Newton's second law for linear motion and Euler's equations for rotational dynamics (Mahony et al., 2012). This formulation captures the interactions between external forces and moments generated by the propellers and the resulting accelerations of the tricopter's center of mass and angular velocity about its principal axes. The rigid body approximation simplifies the analysis while maintaining sufficient accuracy for control design and trajectory planning, enabling a precise representation of the tricopter's behavior during complex maneuvers (Pounds et al., 2010).

### 2.4.1 Kinematic Modeling

The Kinematic equations for the supermaneuverable Tricopter are obtained by using the Transformation from the body frame to the Inertial Fixed frame, is given in equation 1, (Siciliano et al., 2009b):

$$\begin{bmatrix} \dot{X} \\ \dot{Y} \\ \dot{Z} \end{bmatrix} = R \begin{bmatrix} u \\ v \\ w \end{bmatrix}, \quad \begin{bmatrix} \dot{\phi} \\ \dot{\theta} \\ \dot{\psi} \end{bmatrix} = T \begin{bmatrix} p \\ q \\ r \end{bmatrix} \quad (4)$$

Where:

- $x, y, z$  and  $\theta, \phi, \psi$  are translational positions and rotational attitudes, respectively, that are defined in the Fixed Inertia frame.
- $u, v, w$ , and  $p, q, r$  are translational and rotational velocities, respectively, that are defined in the body frame, equations 5 and 6.

$$R = \begin{bmatrix} c\theta c\psi & s\phi s\theta c\psi - s\psi c\phi & c\phi s\theta c\psi + s\phi s\psi \\ c\theta s\psi & s\phi s\theta s\psi + c\psi c\phi & c\phi s\theta s\psi - s\phi c\psi \\ -s\theta & s\phi c\theta & c\phi c\theta \end{bmatrix} \quad (5)$$

$$T = \begin{bmatrix} 1 & s\phi t\theta & c\phi t\theta \\ 0 & c\phi & -s\phi \\ 0 & \frac{s\phi}{c\theta} & \frac{c\phi}{c\theta} \end{bmatrix} \quad (6)$$

Where:

- $R$  is a homogeneous transformation matrix between the Fixed Inertia Frame and Body Frame
- $T$  converts the rotational velocity from the Body frame into the Fixed Inertia Frame.
- $c - \cos, s - \sin, t - \tan$

### 2.4.2 Dynamic Modeling

The following general Newton-Euler equation is used to derive the Linear and rotational acceleration equations 7 and 8, (Murray et al., 1994; Siciliano et al., 2009a):

$$\begin{bmatrix} F_x \\ F_y \\ F_z \end{bmatrix} = m \begin{bmatrix} \dot{u} + (qw - rv) \\ \dot{v} + (ru - pw) \\ \dot{w} + (pv - qu) \end{bmatrix} \quad (7)$$

$$M = Iw + w \times (Iw) \quad (8)$$

Linear acceleration equations 9 to 11:

$$\dot{u} = rv - qw + g\sin(\theta) + \frac{1}{m}F_x, \quad (9)$$

$$\dot{v} = pw - ru - g\sin(\phi)\cos(\theta) + \frac{1}{m}F_y, \quad (10)$$

$$\dot{w} = qu - pv - g\cos(\phi)\cos(\theta) + \frac{1}{m}F_z, \quad (11)$$

Where:

- $F_x, F_y, F_z$  are total external forces acting in the body frame.
- $\theta, \phi$  are pitch and roll angles.

Rotational acceleration equations 12 to 14:

$$\dot{p} = qr \left( \frac{I_{yy} - I_{zz}}{I_{xx}} \right) + \frac{\tau_x}{I_{xx}} \quad (12)$$

$$\dot{q} = pr \left( \frac{I_{zz} - I_{xx}}{I_{yy}} \right) + \frac{\tau_y}{I_{yy}} \quad (13)$$

$$\dot{r} = pq \left( \frac{I_{xx} - I_{yy}}{I_{zz}} \right) + \frac{\tau_z}{I_{zz}} \quad (14)$$

Where:

- $\tau_x, \tau_y, \tau_z$  are total external Moments acting in the body frame.
- $I_{xx}, I_{yy}, I_{zz}$  are the principal moments of Inertia along the Body Frame X-, Y-, Z- axes respectively

In the dynamic modeling of UAV's the aerodynamic thrust force and reactive moment generated by each propeller are commonly expressed as quadratic functions of the propeller's angular velocity (Bouabdallah & Siegwart, 2007; Pounds et al., 2010). Specifically, the thrust force  $F_i$  and the torque  $\tau_x$  produced by the  $i^{th}$  rotor can be modeled as equation 15:

$$F_i = K_f w_i^2, \quad \tau_i = K_m w_i^2 \quad (15)$$

Where:

- $w_i$  denotes the rotor's angular speed of the  $i^{th}$  propeller, and
- $K_f$  and  $K_m$  are the thrust and moment coefficients, respectively.

These coefficients encapsulate the effects of rotor geometry, air density, and blade characteristics, and are typically determined empirically (Floano & Wood, 2015). This quadratic relationship provides a computationally efficient yet physically representative means to model the rotor-generated forces and moments.

The total external forces and moments on the body frame, given in equation 16 and 17:

$$F_{\text{ext}} = \begin{bmatrix} F_x \\ F_y \\ F_z \end{bmatrix} = \begin{bmatrix} F_1 c\beta_1 s\alpha_1 + F_2 c\beta_2 s\alpha_2 + F_3 s\beta_3 \\ F_1 s\beta_1 + F_2 s\beta_2 + F_3 c\beta_3 s\alpha_3 \\ F_1 c\beta_1 c\alpha_1 + F_2 c\beta_2 c\alpha_2 + F_3 c\beta_3 c\alpha_3 \end{bmatrix} \quad (16)$$

$$\tau_{\text{ext}} = \begin{bmatrix} \tau_x \\ \tau_y \\ \tau_z \end{bmatrix}$$

$$\begin{bmatrix} (F_1 c \beta_1 \alpha_1 - F_2 c \beta_2 \alpha_2) L_1 + M_1 c \beta_1 s \alpha_1 + M_2 c \beta_2 s \alpha_2 - M_3 s \beta_3 \\ (F_1 c \beta_1 \alpha_1 + F_2 c \beta_2 \alpha_2) L_2 - F_3 c \beta_3 \alpha_3 L_3 + (M_1 s \beta_1 + M_2 s \beta_2 - M_3 c \beta_3 s \alpha_3) \\ (F_1 c \beta_1 s \alpha_1 - F_2 c \beta_2 s \alpha_2) L_1 + (F_1 s \beta_1 + F_2 s \beta_2) L_2 - F_3 c \beta_3 s \alpha_3 L_3 + M_1 c \beta_1 c \alpha_1 + M_2 c \beta_2 c \alpha_2 - M_3 c \beta_3 c \alpha_3 \end{bmatrix} \quad (17)$$

Where:

- $L_1, L_2, L_3$  - are arm lengths
- $\alpha_1, \alpha_2, \beta_3$  are twisting angles of Propeller 1, 2, and 3 respectively about y-axis
- $\beta_1, \beta_2, \alpha_3$  are twisting angles of Propeller 1, 2, and 3 respectively about x-axis

### 2.4.3 State Space Modeling

The supermaneuverable Tricopter has 12 states, which are the position, orientation, linear velocities, and rotational velocities, depicted in equations 18 and 19:

$$x = [x \ \dot{x} \ y \ \dot{y} \ z \ \dot{z} \ \theta \ \dot{\theta} \ \phi \ \dot{\phi} \ \psi \ \dot{\psi}] \quad (18)$$

The control input vector  $U$  consisting of 6 inputs  $U_1$  through  $U_6$  defined as:

$$U = [U_1 \ U_2 \ U_3 \ U_4 \ U_5 \ U_6] \quad (19)$$

Where:

- $U_1 = F_x, U_2 = F_y, U_3 = F_z, U_4 = \tau_x, U_5 = \tau_y, U_6 = \tau_z$

The equations of motion can be written in state space form by using the following state variables, equations 20 and 21:

$$\dot{x} = f(x, U) \quad (20)$$

$$\dot{x} = [\dot{x} \ \ddot{x} \ \dot{y} \ \ddot{y} \ \dot{z} \ \ddot{z} \ \dot{\theta} \ \ddot{\theta} \ \dot{\phi} \ \ddot{\phi} \ \dot{\psi} \ \ddot{\psi}] \quad (21)$$

## 2.5 Model Predictive Control

For real-time implementation, the nonlinear dynamic model of the Supermaneuverable Tricopter is discretized using numerical integration schemes such as the fourth-order Runge-Kutta (RK4) method or the Euler method, depending on the required balance between computational complexity and accuracy (Rawlings & Q, 2009). This discretized model serves as the basis for forecasting the system's future states during each optimization cycle.

Model Predictive Control (MPC) is an advanced control strategy based on the principles of receding horizon optimal control (Camacho & Bordons, 2007). It is particularly well-suited for systems requiring the simultaneous handling of constraints and performance optimization (Maciejowski, 2002). MPC computes the optimal control input by solving a finite horizon optimization problem at each time step, where the predicted future behavior of the system is optimized over a time window referred to as the prediction horizon (Borrelli, 2003). This prediction is generated using an internal model of the system, and the resulting optimization problem is constrained by system dynamics, actuator limits, and other operational boundaries.

Formally, the MPC problem is posed as a discrete-time constrained finite horizon optimal control problem. The cost function is typically constructed in a least-squares form that penalizes deviations of the predicted state and control trajectories from their respective reference values (Rawlings & Q, 2009). This optimization formulation enables MPC to explicitly account for both control objectives and system limitations within a unified framework, equation 22.

$$\begin{aligned} \min_{x_k, u_k} & \frac{1}{2} \left\{ \sum_{k=j}^{j+N_c-1} \left( \|x_k - x_k^{ref}\|_{w_x}^2 + \|u_k - u_k^{ref}\|_{w_u}^2 \right) + \|x_{N_c} - x_{N_c}^{ref}\|_{w_{N_c}}^2 \right\} \\ \text{s.t.} & \quad x_j = \hat{x}_j \\ & \quad x_{k+1} = f(x_k, u_k), \quad k = j, j+1, \dots, j+N_c-1 \\ & \quad x_{k,min} \leq x_k \leq x_{k,max} \quad k = j, j+1, \dots, j+N_c \end{aligned} \quad (22)$$

$$U_{k,min} \leq U_k \leq U_{k,max} \quad k = j, j + 1, \dots, j + N_c - 1$$

Where:

- $x_k \in \mathcal{R}$ , is the differential state
- $U_k \in \mathcal{R}$ , is the control input
- $\hat{x}_j \in \mathcal{R}$ , is the current state estimate
- $x_k^{ref} \in \mathcal{R}$ , is the reference state
- $u_k^{ref} \in \mathcal{R}$ , is the reference input
- $x_{N_c}^{ref} \in \mathcal{R}$ , is the terminal reference state
- $w_x \in \mathcal{R}$ , is the State Weight matrix
- $w_u \in \mathcal{R}$ , is the input Weight matrix
- $w_{N_c} \in \mathcal{R}$ , is the terminal state Weight matrix
- $x_{k,min}, x_{k,max}$  are the min and max state bound
- $U_{k,min}, U_{k,max}$  are the min and max input bound
- $t_j \leq t \leq t_{j+N_c}$  prediction horizon window

One of the key advantages of MPC lies in its ability to proactively enforce constraints and optimize performance metrics over time, rather than reacting solely to instantaneous deviations (Camacho & Bordons, 2007). Moreover, due to its predictive nature, MPC is capable of generating control actions that anticipate future disturbances or changes in system behavior, thereby improving stability, robustness, and trajectory tracking accuracy in complex and dynamic environments (Borrelli, 2003). These properties make MPC particularly suitable for controlling highly nonlinear and over actuated platforms such as the Supermaneuverable Tricopter, where flexibility, fault tolerance, and precision are critical (Qin et al., 2025; Sheng & Sun, 2016).

### 3. Numerical Result and Discussion

The simulation is done in Simulink by using MPC block as shown in Figure 2 and a MATLAB code generated from the simulation. All the MPC parameters used in this simulation like prediction horizon, Weights, constraints, scenario, and more can be accessed [here](#).

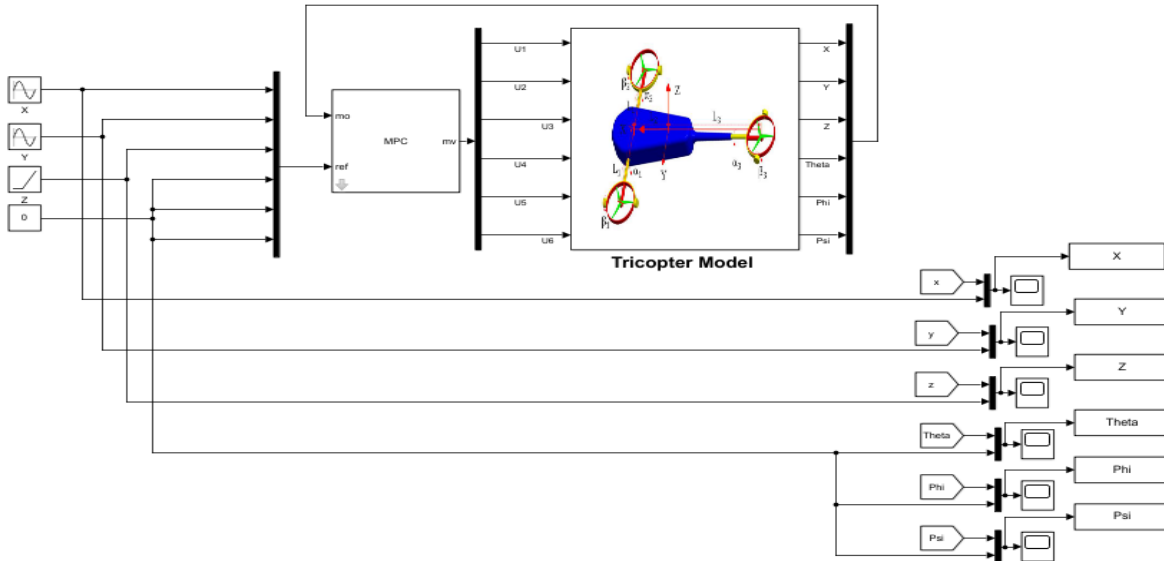


Fig. 2. MPC implementation in Simulink

Figure 3 presents the 3D position tracking results, where the trajectories are followed with high accuracy despite constrained inputs and outputs. Figure 4.a presents the position tracking along the  $x$ -,  $y$ -, and  $z$ -axes, while Figure 4.b shows the forces applied in the  $x$ ,  $y$ , and  $z$ -directions.

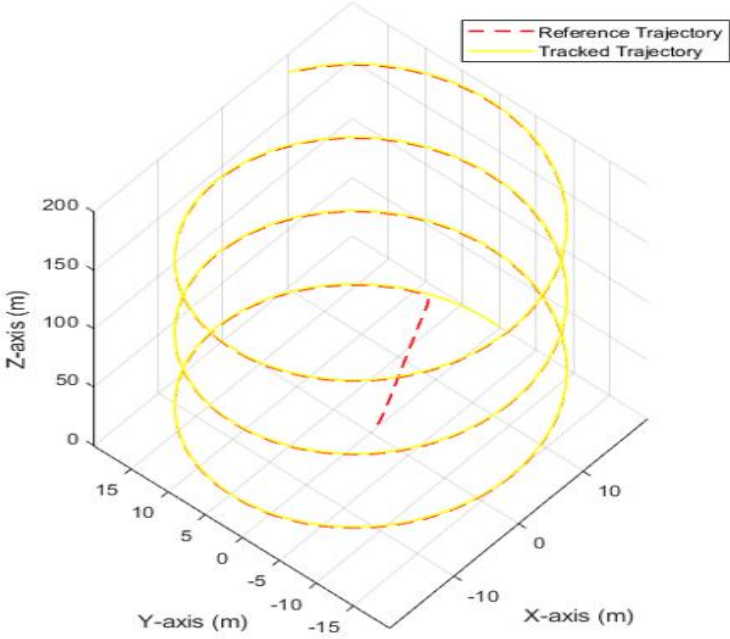
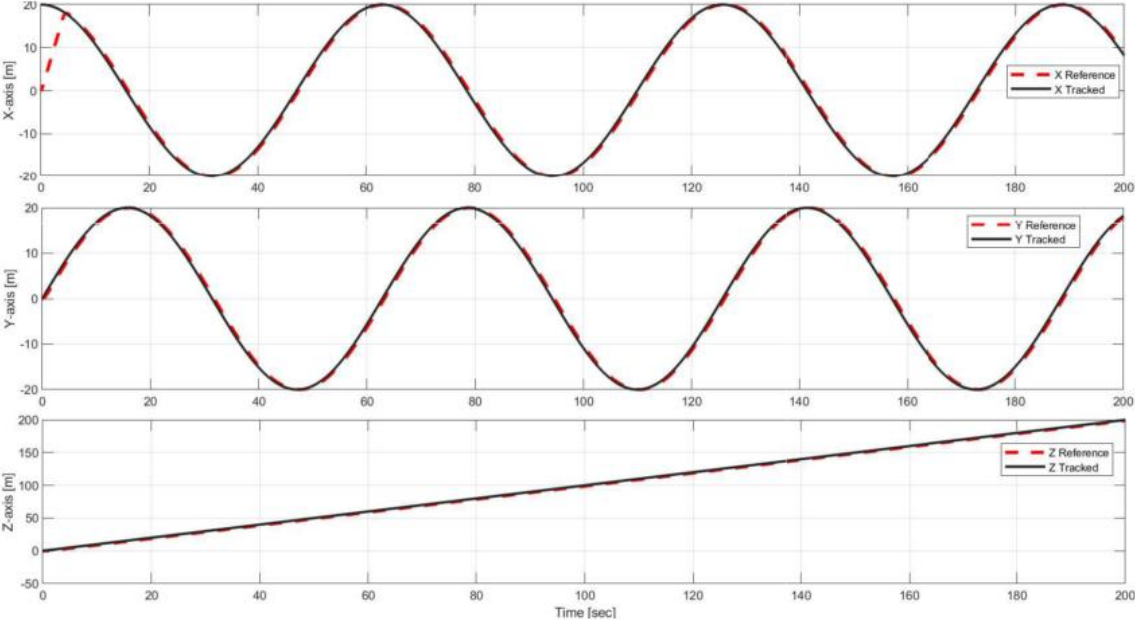
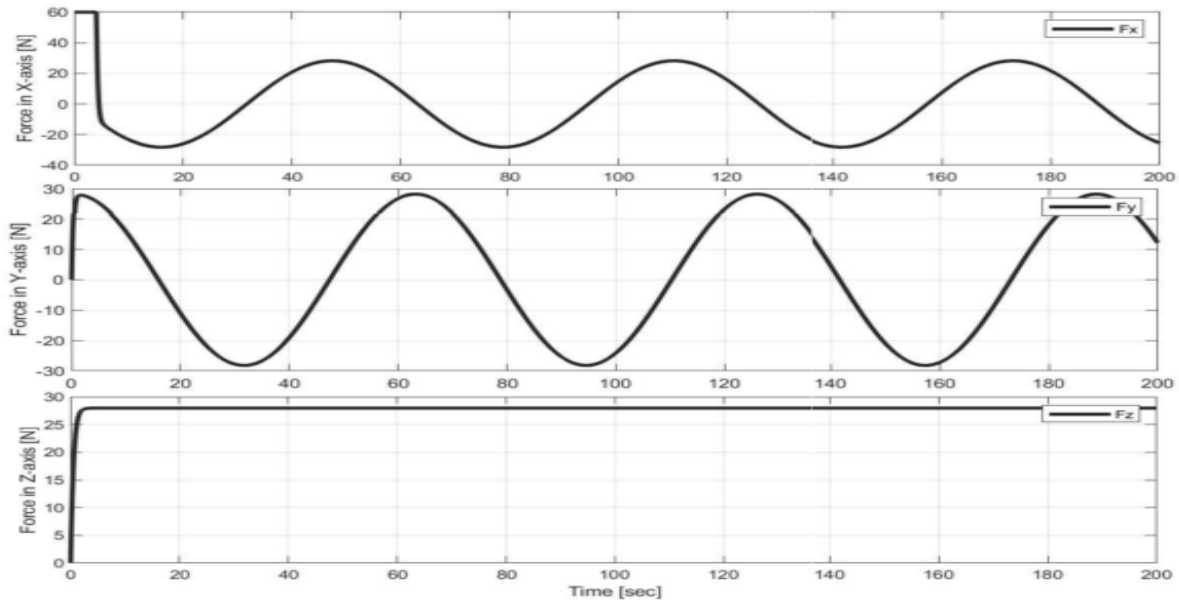


Fig. 3. Position Tracking in 3D





**Fig. 4. a)** Position Tracking in x-axis, y-axis, and z-axis **b)** Forces applied in the x-axis, y-axis, and z-axis

The MPC controller demonstrated high tracking accuracy along the lateral and vertical axes with a maximum overshoot and undershoot of 10 cm along the  $X$ , and  $Y$  axes and with zero over- and undershoot in  $Z$  direction but in a constant delay of 1.2 m in Tracking the reference trajectory as shown in Figure 4.a. All of these simulations are done without leaving the input force constraints of between 60 N and -60 N as shown in figure 4.b. The simulation is done on a 2.5Ghz Core i3 3120M processor with a computational time per control cycle of 9.53 ms, which is around 10ms, for a sampling time of 100 ms used in the simulation demonstrating the controller's computational efficiency and potential to be deployed on embedded platforms.

#### 4. Conclusion

This study presented a novel supermaneuverable Tricopter (SMT) and demonstrated its effective control using an implicit Model Predictive Controller (MPC). This design permits agile maneuvers in all six degrees of freedom without the orientation compromises typical in conventional multirotors. The developed implicit MPC controller was validated through high-fidelity simulation. It achieved high-precision tracking of complex 3D reference trajectories with zero steady-state error, no overshoot, and without invoking unrealistic or excessive control forces or torques. All control actions remained strictly within the physical and actuator constraints of the system. The MPC framework successfully leveraged the platform's actuation redundancy to ensure smooth, optimal, and constraint-compliant performance across a wide range of dynamic maneuvers. Moreover, the controller's low computational footprint enables direct deployment in real-time embedded applications without the need to reformulate the implicit MPC into an explicit form.

#### References

- Abara, D., Kannan, S., & Lanson, A. (2020). Development and stabilization of a low-cost single-tilt tricopter\*. *IFAC-PapersOnLine*, 53(2), 8897–8902. <https://doi.org/10.1016/j.ifacol.2020.12.1411>
- Arroyo, A. D. H., Morais, A. S., Lima, G. V., & Ribeiro, L. (2021). Modeling and Simulation of a Novel Tilt-Wing-Coaxial-Rotor Tricopter. *Simpósio Brasileiro de Automação Inteligente - SBAI*, 1(1), Article 1. <https://doi.org/10.20906/sbai.v1i1.2627>

- Barua, P., & Maneeshwar, P. (n.d.). *Problems Associated with the Stability of Bicopters and Tricopters* (No. 02). 42(02), Article 02.
- Borrelli, F. (Ed.). (2003). Constrained Optimal Control for Hybrid Systems. In *Constrained Optimal Control of Linear and Hybrid Systems* (pp. 143–171). Springer. [https://doi.org/10.1007/3-540-36225-8\\_8](https://doi.org/10.1007/3-540-36225-8_8)
- Bouabdallah, S., & Siegwart, R. (2007, October). Full control of a quadrotor. *2007 IEEE/RSJ International Conference on Intelligent Robots and Systems*. 2007 IEEE/RSJ International Conference on Intelligent Robots and Systems, San Diego, CA, USA. <https://doi.org/10.1109/iroso.2007.4399042>
- Camacho, E. F., & Bordons, C. (2007). Introduction to Model Predictive Control. In E. F. Camacho & C. Bordons (Eds.), *Model Predictive control* (pp. 1–11). Springer. [https://doi.org/10.1007/978-0-85729-398-5\\_1](https://doi.org/10.1007/978-0-85729-398-5_1)
- Chen, Z., & Jia, H. (2020). Design of Flight Control System for a Novel Tilt-Rotor UAV. *Complexity*, 2020(1), Article 1. <https://doi.org/10.1155/2020/4757381>
- Cortés, J., & Egerstedt, M. (2017). Coordinated Control of Multi-Robot Systems: A Survey. *SICE Journal of Control, Measurement, and System Integration*, 10(6), Article 6. <https://doi.org/10.9746/jcmsi.10.495>
- Ding, C., & Lu, L. (2021). A Tilting-Rotor Unmanned Aerial Vehicle for Enhanced Aerial Locomotion and Manipulation Capabilities: Design, Control, and Applications. *IEEE/ASME Transactions on Mechatronics*, 26(4), 2237–2248. <https://doi.org/10.1109/TMECH.2020.3036346>
- Floreano, D., & Wood, R. J. (2015). Science, technology and the future of small autonomous drones. *Nature*, 521(7553), Article 7553. <https://doi.org/10.1038/nature14542>
- Hao, W., Xian, B., & Xie, T. (2022). Fault-Tolerant Position Tracking Control Design for a Tilt Tri-Rotor Unmanned Aerial Vehicle. *IEEE Transactions on Industrial Electronics*, 69(1), 604–612. <https://doi.org/10.1109/TIE.2021.3050384>
- Kunertova, D. (2024). *Learning from the Ukrainian Battlefield: Tomorrow's Drone Warfare, Today's Innovation Challenge* (p. 27 p.) [Application/pdf]. ETH Zurich. <https://doi.org/10.3929/ETHZ-B-000690448>
- Landry, B., Deits, R., Florence, P. R., & Tedrake, R. (2016). Aggressive quadrotor flight through cluttered environments using mixed integer programming. *2016 IEEE International Conference on Robotics and Automation (ICRA)*, 1469–1475. <https://doi.org/10.1109/icra.2016.7487282>
- Maclejowski, J. M. (2002). *Predictive Control With Constraints*. Pearson College Div.
- Mahony, R., Kumar, V., & Corke, P. (2012). Multirotor aerial vehicles: Modeling, estimation, and control of quadrotor. *IEEE Robotics and Automation Magazine*, 19(3), Article 3. <https://doi.org/10.1109/MRA.2012.2206474>
- Mehndiratta, M., & Kayacan, E. (2018). Reconfigurable Fault-tolerant NMPC for Y6 Coaxial Tricopter with Complete Loss of One Rotor. *2018 IEEE Conference on Control Technology and Applications (CCTA)*, 774–780. <https://doi.org/10.1109/CCTA.2018.8511444>
- Michael, N., Mellinger, D., Lindsey, Q., & Kumar, V. (2010). The GRASP Multiple Micro-UAV Testbed. *IEEE Robotics & Automation Magazine*, 17(3), Article 3. <https://doi.org/10.1109/mra.2010.937855>
- Mohamed, M. K., & Lanzon, A. (2012a). Design and control of novel tri-rotor UAV. *Proceedings of 2012 UKACC International Conference on Control*, 304–309. <https://doi.org/10.1109/control.2012.6334647>
- Mohamed, M. K., & Lanzon, A. (2012b). Design and control of novel tri-rotor UAV. *Proceedings of 2012 UKACC International Conference on Control*, 304–309. <https://doi.org/10.1109/control.2012.6334647>
- Mohanty, S. N., Ravindra, J. V. R., Narayana, G. S., Pattnaik, C. R., & Sirajudeen, Y. M. (2023). *Drone Technology: Future Trends and Practical Applications*. John Wiley & Sons.
- Murray, R. M., Li, Z., Sastry, S. S., & Sastry, S. S. (1994). *A Mathematical Introduction to Robotic Manipulation*. CRC Press.

- Nam, K.-J., Joung, J., & Har, D. (2020). Tri-Copter UAV With Individually Tilted Main Wings for Flight Maneuvers. *IEEE Access*, 8, 46753–46772. <https://doi.org/10.1109/access.2020.2978578>
- Peksa, J., & Mamchur, D. (2024). A Review on the State of the Art in Copter Drones and Flight Control Systems. *Sensors*, 24(11), Article 11. <https://doi.org/10.3390/s24113349>
- Pounds, P., Mahony, R., & Corke, P. (2010). Modelling and control of a large quadrotor robot. *Control Engineering Practice*, 18(7), Article 7. <https://doi.org/10.1016/j.conengprac.2010.02.008>
- Qin, C., Zhao, N., Wang, Q., Luo, Y., & Shen, Y. (2025). Minimum Snap Trajectory Planning and Augmented MPC for Morphing Quadrotor Navigation in Confined Spaces. *Drones*, 9(4), Article 4. <https://doi.org/10.3390/drones9040304>
- Rawlings, J. B., & Q, M. D. (2009). *Model Predictive Control Theory and Design*. Nob Hill Pub, Llc.
- Sai, S. K. (n.d.). *Modeling and Analysis of Tri-Copter (VTOL) Aircraft*.
- Sheng, S., & Sun, C. (2016). Control and Optimization of a Variable-Pitch Quadrotor with Minimum Power Consumption. *Energies*, 9(4), Article 4. <https://doi.org/10.3390/en9040232>
- Siciliano, B., Sciavicco, L., Villani, L., & Oriolo, G. (Eds.). (2009a). Dynamics. In *Robotics: Modelling, Planning and Control* (pp. 247–302). Springer. [https://doi.org/10.1007/978-1-84628-642-1\\_7](https://doi.org/10.1007/978-1-84628-642-1_7)
- Siciliano, B., Sciavicco, L., Villani, L., & Oriolo, G. (Eds.). (2009b). Kinematics. In *Robotics: Modelling, Planning and Control* (pp. 39–103). Springer. [https://doi.org/10.1007/978-1-84628-642-1\\_2](https://doi.org/10.1007/978-1-84628-642-1_2)
- Tahir, M., Aamir, M., Rajper, S. A., & Kumar, R. (2025). Future Implications of the Drone Industry: Emerging Trends and Potential Challenges. In *Computer Vision and Edge Computing Technologies for the Drone Industry* (pp. 167–182). IGI Global Scientific Publishing. <https://doi.org/10.4018/979-8-3693-8497-8.ch007>
- Valsan, A., B., P., G. H., V. D., Unnikrishnan, R. S., Reddy, P. K., & A., V. (2020). Unmanned Aerial Vehicle for Search and Rescue Mission. *2020 4th International Conference on Trends in Electronics and Informatics (ICOEI)(48184)*, 684–687. <https://doi.org/10.1109/ICOEI48184.2020.9143062>